

Original Article

Inhibition of MyD88 by a novel inhibitor reverses two-thirds of the infarct area in myocardial ischemia and reperfusion injury

Yan Miao^{1,3}, Zuochuan Ding⁴, Zhimiao Zou^{1,3}, Yang Yang^{1,3}, Min Yang², Xiaoqian Zhang⁵, Zeyang Li^{1,3}, Liang Zhou^{1,3}, Limin Zhang^{1,3}, Xue Zhang⁷, Dunfeng Du^{1,3}, Fengchao Jiang⁶, Ping Zhou^{1,3}

¹Institute of Organ Transplantation, ²Department of Pediatrics, Tongji Hospital, Tongji Medical College, Huazhong University of Science and Technology, Wuhan, China; ³Key Laboratory of Organ Transplantation, Ministry of Education, NHC Key Laboratory of Organ Transplantation, Key Laboratory of Organ Transplantation, Chinese Academy of Medical Sciences, Wuhan, China; ⁴Department of General Surgery, The First Affiliated Hospital of Nanchang University, Nanchang, China; ⁵Department of Neurology, Union Hospital, ⁶Academy of Pharmacy, Tongji Medical College, Huazhong University of Science and Technology, Wuhan, China; ⁷Department of Breast Surgery, Renmin Hospital of Wuhan University, Wuhan University, Wuhan, China

Received January 3, 2020; Accepted July 15, 2020; Epub September 15, 2020; Published September 30, 2020

Abstract: Cardiomyocytes, macrophages, and fibroblasts play important roles in inflammation and repair during myocardial ischemia/reperfusion injury (MIRI). Myeloid differentiation primary response 88 (MyD88) is upregulated in immunocytes, cardiomyocytes, and fibroblasts during MIRI. MyD88 induces the secretion of proinflammatory cytokines, including interleukin (IL)-1 β , IL-6, and tumor necrosis factor alpha (TNF- α), while fibroblasts are recruited and activated to mediate cardiac remodeling. The aim of this study was to assess the anti-MIRI effect and mode of action of the novel MyD88 inhibitor TJ-M2010-5. We synthesized TJ-M2010-5 and identified its target by co-immunoprecipitation, after which we established a murine MIRI model and tested the protective effect of TJ-M2010-5 by immunohistochemistry, flow cytometry, real-time PCR, and western blotting. Neonatal rat cardiomyocytes subjected to anoxia/reoxygenation were also isolated and their supernatants used to stimulate cardiac macrophagocytes and fibroblasts *in vitro*. MyD88 was found upregulated during the early and late phases after MIRI. The MyD88 inhibitor considerably improved cardiac function, reduced cardiomyocyte apoptosis, reduced IL-1 β , IL-6, and TNF- α secretion, and inhibited CD80+CD86+MHCII+ macrophage and fibroblast migration. Moreover, TJ-M2010-5 markedly inhibited Toll-like receptor/MyD88 signaling *in vivo* and *in vitro*. Thus, our findings highlight TJ-M2010-5 as a potential therapeutic agent for MIRI treatment.

Keywords: Anoxia/reoxygenation, myeloid differentiation factor 88, myocardial ischemia and reperfusion injury, remodeling, TJ-M2010-5

Introduction

Acute myocardial infarction is a life-threatening condition. Some 4.5 million cases are reported in China alone, with the number increasing each year. Coronary artery recirculation is the only effective treatment [1-3]; however, severe reperfusion injury following this intervention may contribute to more than half of the infarct area, cause inflammation, and remodel the ventricles. Collectively, these symptoms constitute myocardial ischemia reperfusion injury (MIRI) [4]. Although MIRI is heavily researched, there is still a lack of an effective treatment strategy.

Toll-like receptors (TLRs) are associated with the innate immune response, which is critical for MIRI [5]. TLR2 and TLR4 are expressed in immunocytes, cardiomyocytes, and fibroblasts, which play a key role in inflammation and repair [6-8]. During MIRI, massive cardiomyocyte necrosis occurs when TLRs recognize danger-associated molecular patterns (DAMPs), such as the proinflammatory chemokines interleukin (IL)-6, IL-1 β , and tumor necrosis factor-alpha (TNF- α). Neutrophils and monocytes are extravasated to the ischemic area to trigger inflammatory responses [6, 8]. Fibroblasts migrate to the ischemic area, where they are activated to suppress inflammation. Consequently, patho-

logical cardiac remodeling occurs [9, 10]. TLRs, except for TLR3, may fully respond via the adaptor myeloid differentiation primary response 88 (MyD88) protein, while others, such as TLR2 and TLR4, may partially respond in combination with the adaptor Toll interleukin-1 receptor (TIR) domain-containing adaptor protein (TIRAP) [8, 11]. Therefore, therapeutic targeting of MyD88 signaling, MyD88-mediated cells and inflammatory mediators may confer protection against MIRI.

MyD88 comprises an *N*-terminal death domain and a *C*-terminal TIR domain separated by a short linker region [12]. MyD88 activation induces downstream interleukin-1 receptor-associated kinase phosphorylation. MyD88 interacts with TNF receptor-associated factor 6 (TRAF6), which activates the downstream nuclear factor kappa-light-chain-enhancer of activated B cells (NF- κ B) and mitogen-activated protein kinase (MAPK) pathways [13-15]. These signals promote the expression of co-stimulatory molecules, such as CD80, CD86, and major histocompatibility complex class II (MHCII), to induce an acquired immune response [16]. Simultaneously, fibroblasts respond to the aforementioned chemokines and cytokines and migrate to the ischemic area. This mechanism is closely associated with poor left ventricular remodeling and heart failure during later stages of MIRI [9].

Here, we synthesized TJ-M2010-5 (WIPO patent application number, PCT/CN2012/070-811), which specifically interacts with the MyD88 TIR domain and interferes with MyD88 dimerization. Previously, we found that TJ-M2010-5 is efficacious in the treatment of cardiac and skin graft rejection, acute liver injury, and colitis-associated colorectal cancer [17-19].

In this study, the relative efficacy of TJ-M2010-5 was tested using a murine model of myocardial ischemia and an *in vitro* reperfusion injury and anoxia/reoxygenation (A/R) experiment. We show that MyD88 is largely expressed on cardiomyocytes, cardiac macrophages, and fibroblasts. We also demonstrate that TJ-M2010-5 protects the heart from MIRI by reducing the infarct area by nearly two-thirds and reducing cardiomyocyte apoptosis, proinflammatory neutrophil infiltration, and the activation and migration of macrophages and fibroblasts.

Materials and methods

The data, analytical methods, and study materials can be obtained directly from the corresponding authors upon reasonable request. All other supporting data are available within the article and in the Online Supplement.

Chemical structure and target of TJ-M2010-5

TJ-M2010-5, 3-(4-(4-benzylpiperazin-1-yl)-*N*-(4-phenylthiazol-2-yl)) propenamide (**Figure 1A**), was synthesized at the Academy of Pharmacy, Huazhong University of Science and Technology, Wuhan, China (WIPO patent application number, PCT/CN2012/070811). TJ-M2010-5 was dissolved in distilled deionized water (ddH₂O) and its structure and purity were established by nuclear magnetic resonance and high-performance liquid chromatography as previously described [19]. Its interaction with the MyD88 TIR domain is illustrated in **Figure 1B**.

Plasmids, cell culture, transfection, and co-immunoprecipitation assay

The full sequence length-expressing plasmids pcDNA3.1-(Flag-MyD88) for FLAG-tagged MyD88, pcDNA3.1-(HA-MyD88) for HA-tagged MyD88, pcDNA3.1-(Flag-TIRAP) for FLAG-tagged TIRAP, pcDNA3.1-(Flag-con) for FLAG-tagged control, and pcDNA3.1-(HA-con) for HA-tagged control were generated by Shanghai GeneChem. Co. Ltd. (Shanghai, China). The FLAG-con and HA-con plasmids lacked the MyD88 (NM_002468) and TIRAP (NM_054096) sequences. H9C2 cells (Cell Bank of the Committee of Type Culture Collection of the Chinese Academy of Sciences, Shanghai, China) were cultured in Dulbecco's modified Eagle's medium (DMEM; Gibco, Thermo Fisher Scientific, Waltham, MA) supplemented with 10% (w/v) fetal bovine serum (FBS; Gibco) in a 37°C humidified atmosphere under 5% CO₂. The cells were co-transfected with 4 μ g of HA-MyD88/Flag-MyD88 or HA-MyD88/Flag-TIRAP using Lipofectamine™ 2000 (Invitrogen, Carlsbad, CA). After 6 h, the cells were treated with various concentrations of TJ-M2010-5 (0, 15, or 30 μ mol/L). After 48 h, cells were harvested and lysed in radioimmunoprecipitation assay buffer (Beyotime Institute of Biotechnology, Shanghai, China). Cell lysates were collected for immunoprecipitation on pro-

MyD88 inhibitor attenuates MIRI

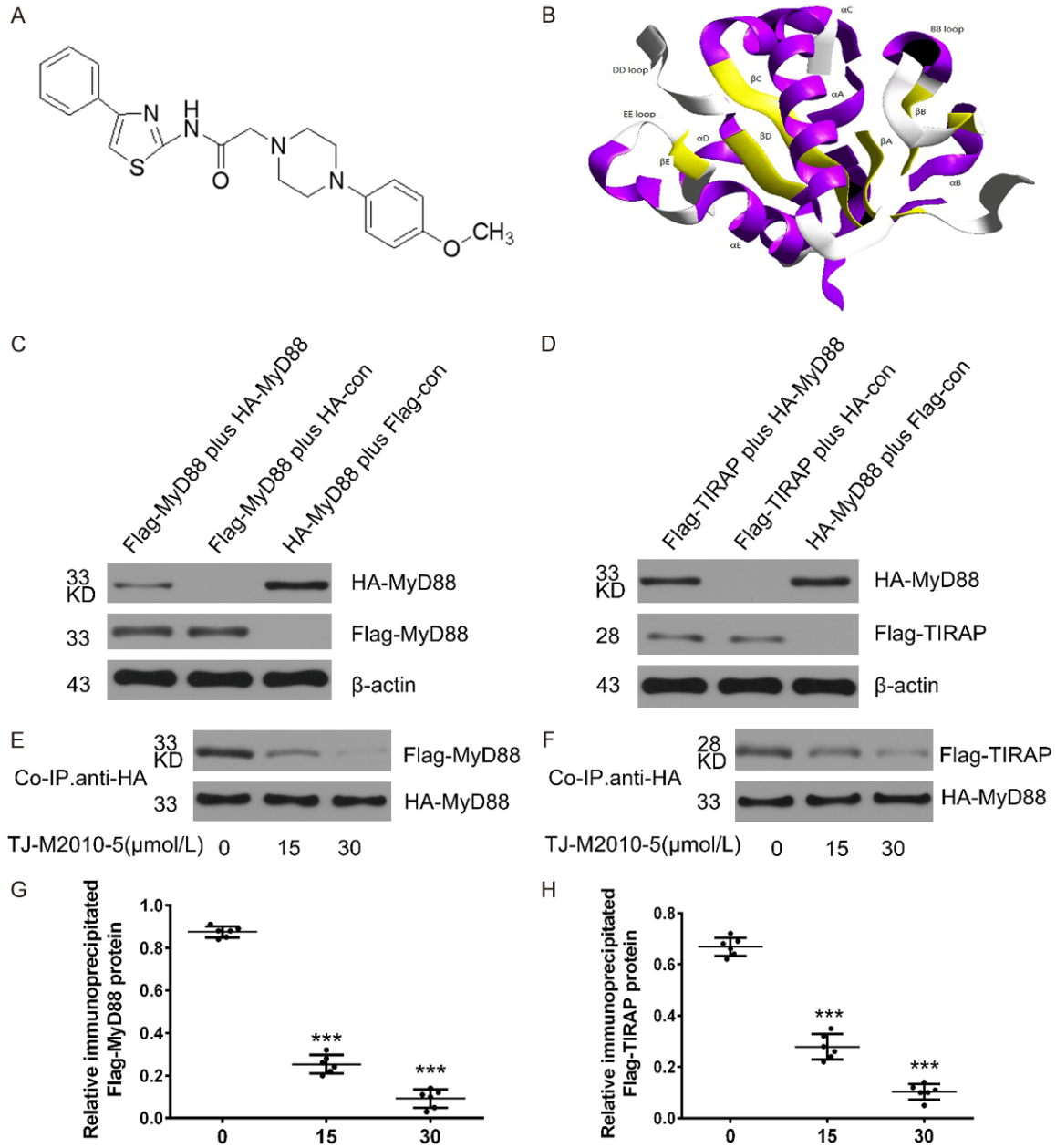


Figure 1. Molecular structure of MyD88 and its interaction with the MyD88 TIR domain. A. Structure of TJ-M2010-5. B. TJ-M2010-5 enters the molecular structure of the TIR MyD88 domain via αE (box 3) and binds to the amino acid residues of αE , βD , βC , and αA , as well as the death domain and EE loops of MyD88. C, D. FLAG-MyD88, HA-MyD88, and FLAG-TIRAP proteins were successfully expressed in the system and confirmed by anti-FLAG or anti-HA antibodies. β -actin served as control. E, F. Co-immunoprecipitation demonstrated that groups transfected with FLAG-MyD88 + HA-MyD88 and FLAG-TIRAP + HA-MyD88 successfully formed stable dipolymers in H9C2 cells ($n = 6$; one of three independent experiments). TJ-M2010-5 inhibited MyD88 dimerization in a dose-dependent manner. The level of dimerized MyD88 was normalized to untreated controls. G, H. Densitometry of co-immunoprecipitation assays. The density of each HA-MyD88 signal was divided by that of FLAG-MyD88. Data represent the means \pm SD; *** $P < 0.001$ vs. 0 μ mol/L TJ-M2010-5; one-way ANOVA with Dunnett's post-hoc test.

tein A/G agarose beads (Thermo Fisher Scientific). Immunocomplexes captured on the protein beads were eluted in SDS-PAGE sample buffer for western blotting.

Mice and ethics approval

Male C57BL/6 mice (6-8 weeks; Human SJA Laboratory Animal Company, Changsha, China)

MyD88 inhibitor attenuates MIRI

and C57BL/6 MyD88^{-/-} mice (generously provided by Dr. Maria-Luisa Alegre at the University of Chicago, Chicago, IL) were housed in a specific pathogen-free facility and maintained under controlled conditions (21-23°C, 55-60% humidity, 12-h day/night cycle) at the Huazhong University of Science and Technology, Wuhan, China. C57BL/6 MyD88^{-/-} mice were crossed with C57BL/6 WT mice for three generations and genotyped according to established protocols. All animals were acclimatized for one week before the experiments. All study procedures were approved by the Animal Care and Research Committee of Huazhong University of Science and Technology and conform to the Guidelines on the Care and Use of Animals for Scientific Purposes by Hubei Province and Huazhong University of Science and Technology laboratory animal ethics committee; the guidelines from Directive 2010/63/EU of the European Parliament on the protection of animals used for scientific purposes; and the Guide for the Care and Use of Laboratory Animals published by the US National Institutes of Health (NIH Publication, 8th Edition, 2011).

In vivo MIRI protocol and treatment

Myocardial ischemia and reperfusion were induced as previously described [20]. Briefly, mice were intubated, ventilated with a rodent ventilator, and maintained under anesthesia with 1.0-2.0% isoflurane gas. Left thoracotomies were performed, and the left anterior descending coronary arteries (visible on the left or at the lower margin of the left atrial appendage) were ligated by tying slipknots with a 7-0 silk suture around PE-10 tubing. When the anterior walls of the left ventricles (LVs) became cyanotic and local contractile movements were restricted, myocardial ischemia was successfully induced. After 30 min, reperfusion was permitted for various times by untying the slipknots. Sham-operated animals were subjected to the aforementioned surgical procedures except that the sutures were passed under the left anterior descending arteries without being tied. Mice were divided into the following four groups: (1) sham (control) group, where mice were subjected to intraperitoneal injection (i.p.) with ddH₂O (50 mg/kg); (2) ddH₂O group, where mice were injected with ddH₂O (50 mg/kg, i.p.) as a positive control plus an equal volume of TJ-M-2010-5; (3) TJ-M2010-5 group, where mice were injected with TJ-M2010-5 (50 mg/

kg, i.p.); and (4) MyD88^{-/-} group, where mice were injected with ddH₂O (50 mg/kg, i.p.). All groups were treated once daily for 2 d before surgery.

Isolation and verification of neonatal rat cardiomyocytes and fibroblasts

Cardiomyocytes and fibroblasts from 1-day-old C57BL/6 mice (Hubei Research Center for Laboratory Animals, Wuhan, China) were prepared as previously described [21]. Briefly, animals were anesthetized with 1.0-2.0% isoflurane gas and then ventricles were minced and digested with pancreatin (0.8 mg/mL) and collagenase type 2 (1 mg/mL; Sigma-Aldrich, St. Louis, MO) in D-Hanks Balanced Salt Solution (8.00 g NaCl, 30.35 g NaHCO₃, 0.37 g Na₂HPO₄·12H₂O, 0.40 g KCl, and 0.06 g KH₂PO₄) in a shaking water bath (800 rpm, 37°C). Cells were collected by centrifugation (300 ×g, 5 min, 21-25°C), resuspended in plating medium (90% DMEM, 10% [w/v] FBS, and 100 U/mL penicillin + streptomycin) in 95% air and 5% CO₂ at 37.5°C. After 2 h, adherent fibroblasts and non-adherent cardiomyocytes were present in the supernatant. The non-adherent cardiomyocytes were collected and cultured in serum-free maintenance medium (90% DMEM, 10% [w/v] FBS, 1% [w/v] bromodeoxyuridine [BrdU], and 100 U/mL penicillin + streptomycin) for 2 d. The medium was then replaced with fresh serum-free maintenance medium without BrdU. Primary cardiomyocytes and fibroblasts underwent two passages and were verified by immunofluorescence with mouse monoclonal anti-cardiac troponin T (1:100; cat. GB11364; Servicebio, Wuhan, China) and mouse monoclonal anti-vimentin (1:200; cat. GB14167; Servicebio).

A/R protocol and treatment

After 5 d, cardiomyocytes were divided into four groups consisting of control and three A/R + TJ-M2010-5 groups (A/R + 0 μmol/L TJ-M2010-5, A/R + 5 μmol/L TJ-M2010-5, A/R + 15 μmol/L TJ-M2010-5, and A/R + 30 μmol/L TJ-M2010-5, respectively) and incubated for 12 h. The medium was then replaced with serum-free medium and subjected to anoxia in a chamber atmosphere of 95% N₂ and 5% CO₂ for 4 h. The cells were then returned to an incubator atmosphere of 95% air and 5% CO₂ for 2 h. For the control normoxic groups, cells were

MyD88 inhibitor attenuates MIRI

incubated with fresh culture growth medium under 95% air and 5% CO₂ for 6 h. The supernatants and cardiomyocytes were then harvested for use in subsequent experiments.

Bone marrow-derived macrophage (BMDM) culture and intervention

Male C57BL/6 mice (6-8-week-old) were euthanized with overdose ketamine (225 mg/kg) and medetomidine (3 mg/kg), after which the tibial and femoral bones were dissected from the mice under a sterile environment. Bone marrow cells were collected in 1 mL phosphate-buffered saline, incubated with 3 mL red blood cell lysis solution (Beyotime Institute of Biotechnology) at 4°C for 10-20 min, and cultured in 6-well plates at a density of 1×10⁶ cells/mL with 2 mL of a mixture containing 90% (w/v) DMEM, 10% (w/v) FBS, 100 U/mL penicillin + streptomycin, and 20 ng/mL macrophage colony-stimulating factor (M-CSF; Peprotech, London, UK). On day 3, the culture medium was replaced with fresh medium and supplemented with 20 ng/mL M-CSF. On day 6, the macrophages were divided into five groups consisting of control and four A/R cardiomyocyte supernatant + TJ-M2010-5 groups (macrophages + A/R + 0 μmol/L TJ-M2010-5, macrophages + A/R + 5 μmol/L TJ-M2010-5, macrophages + A/R + 15 μmol/L TJ-M2010-5, and macrophages + A/R + 30 μmol/L TJ-M2010-5, respectively). The groups were treated with TJ-M2010-5 or ddH₂O for 12 h before stimulation with the A/R cardiomyocyte supernatant. After 12 h, the supernatants and BMDMs were harvested for use in subsequent experiments.

Statistical analysis

Data are represented as the means ± standard deviation (SD). Paired comparisons were performed using Student's *t*-test. Multiple group comparisons were performed using one-way ANOVA followed by Dunnett's test. *P* < 0.05 was considered statistically significant. Statistical analyses were performed using GraphPad Prism version 6.02 (GraphPad Software Inc., La Jolla, CA) and SPSS version 15.0 for Windows (SPSS Inc., Chicago, IL).

Additional methods

The expanded methods section in the online-only data supplement contains information on

cardiac enzymes, echocardiography, infarct size assessment, hematoxylin and eosin (H&E) staining, terminal deoxynucleotidyl transferase-mediated nick-end labeling (TUNEL) assay, immunohistochemistry (IHC), immunofluorescence, Masson's trichrome staining, flow cytometry (FCM) analysis, real-time reverse transcription polymerase chain reaction (qRT-PCR), western blotting, enzyme-linked immunosorbent assay (ELISA), and Transwell migration assays.

Results

TJ-M2010-5 inhibits MyD88-MyD88 homodimerization and TIRAP-MyD88 heterodimerization

Four different plasmids were transfected into H9C2 cells to express MyD88 and assess its dimerization (**Figure 1C** and **1D**). We then performed co-immunoprecipitation assays to determine whether various concentrations of TJ-M2010-5 can bind MyD88 monomers and found that TJ-M2010-5 inhibited MyD88 dimerization in a dose-dependent manner (**Figure 1E-H**).

MyD88 is significantly upregulated in mouse heart tissues subjected to induced MIRI, A/R-induced cardiomyocytes, and macrophagocytes and fibroblasts stimulated by the supernatants of A/R-treated cardiomyocytes

We investigated MyD88 expression in different cell types of the myocardium and at various reperfusion time points after MIRI. Double- and triple-immunofluorescence analyses revealed that nearly all MyD88-expressing cardiac cells were α-actinin+ and F4/80+ on day 1 after MIRI and vimentin+ on day 28 after ischemia reperfusion. However, Ly-6G+ cells rarely expressed MyD88 (**Figure 2A**). MyD88 mRNA levels were significantly increased as soon as 2 h after reperfusion and continued to increase until 28 d after reperfusion (**Figure 2B**). Moreover, western blotting using heart tissues of mice with induced MIRI, A/R-treated cardiomyocytes, and macrophagocytes and fibroblasts stimulated by the supernatants of A/R-treated cardiomyocytes confirmed that MyD88 was substantially upregulated in the treatment groups compared with control (**Figure 2C-F**).

MyD88 inhibitor attenuates MIRI

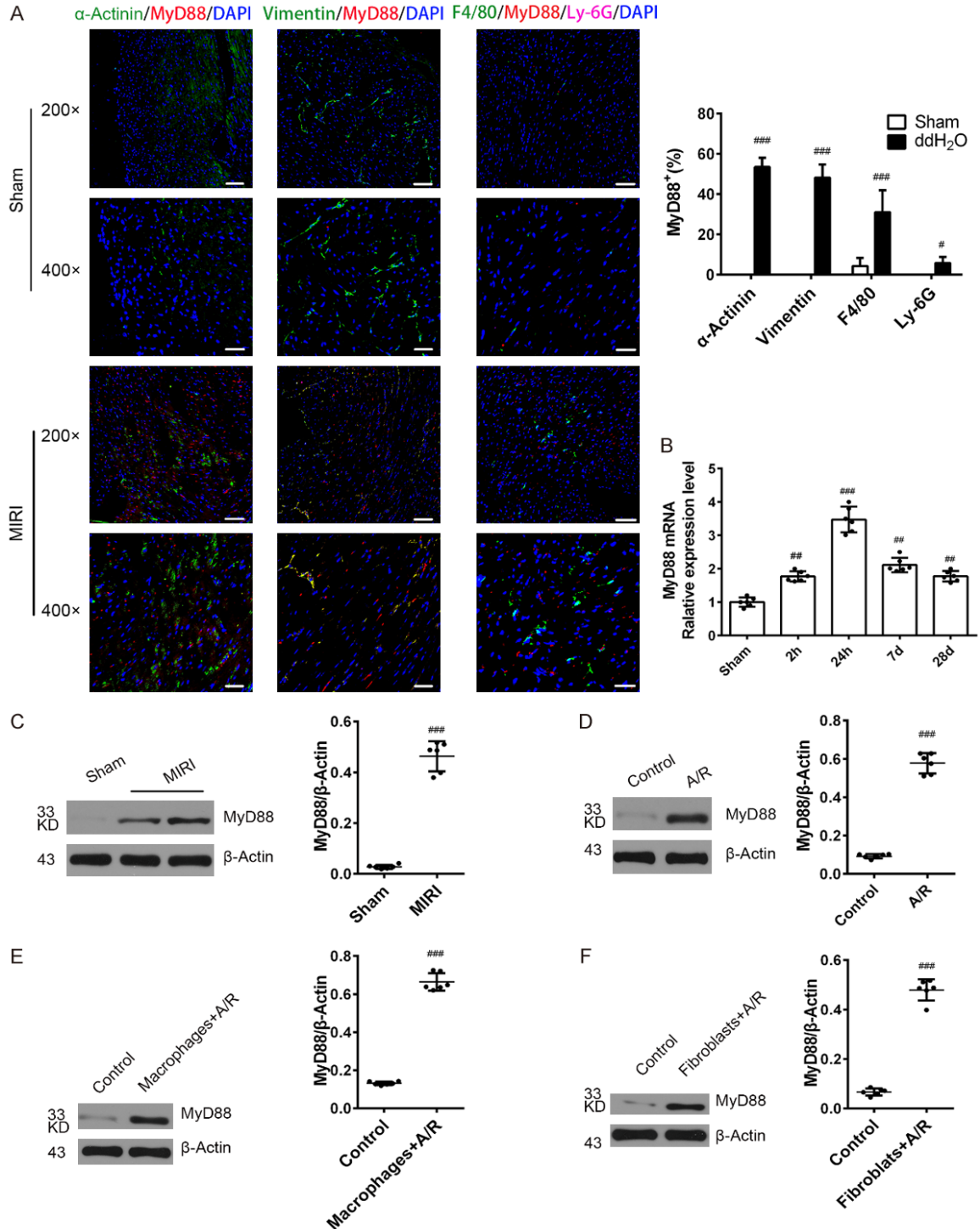


Figure 2. MyD88 is significantly upregulated in MIRI mouse heart tissues, A/R-induced cardiomyocytes, and macrophagocytes and fibroblasts stimulated with supernatants of A/R-exposed cardiomyocytes. (A) Representative immunofluorescence staining of MyD88, α-actinin, F4/80, Ly-6G, and vimentin in murine heart 24 h after ischemia reperfusion (n = 6). Original magnification, 200× (top panel); scale bar = 50 μm. Magnified view, 400× (bottom panel); scale bar = 25 μm. (B) MyD88 mRNA levels measured by qRT-PCR and based on total RNA extracted from heart tissues (n = 6). (C-F) Western blotting showing MyD88 expression in total protein extracts from heart tissues, A/R-induced cardiomyocytes, macrophagocytes and fibroblasts stimulated by the supernatants of A/R-treated cardiomyocytes (n = 6; representative data for one of three independent experiments are shown). Band densities were digitized and semi-quantified. Density of the β-actin signal was divided by that of MyD88. Data represent the means ± SD. **P* < 0.01, ***P* < 0.01, ****P* < 0.001 vs. sham (A-C); *****P* < 0.001 vs. control (D-F); one-way ANOVA with Dunnett's post-hoc test (A, B) and Student's *t*-test (C-F).

MyD88 inhibitor attenuates MIRI

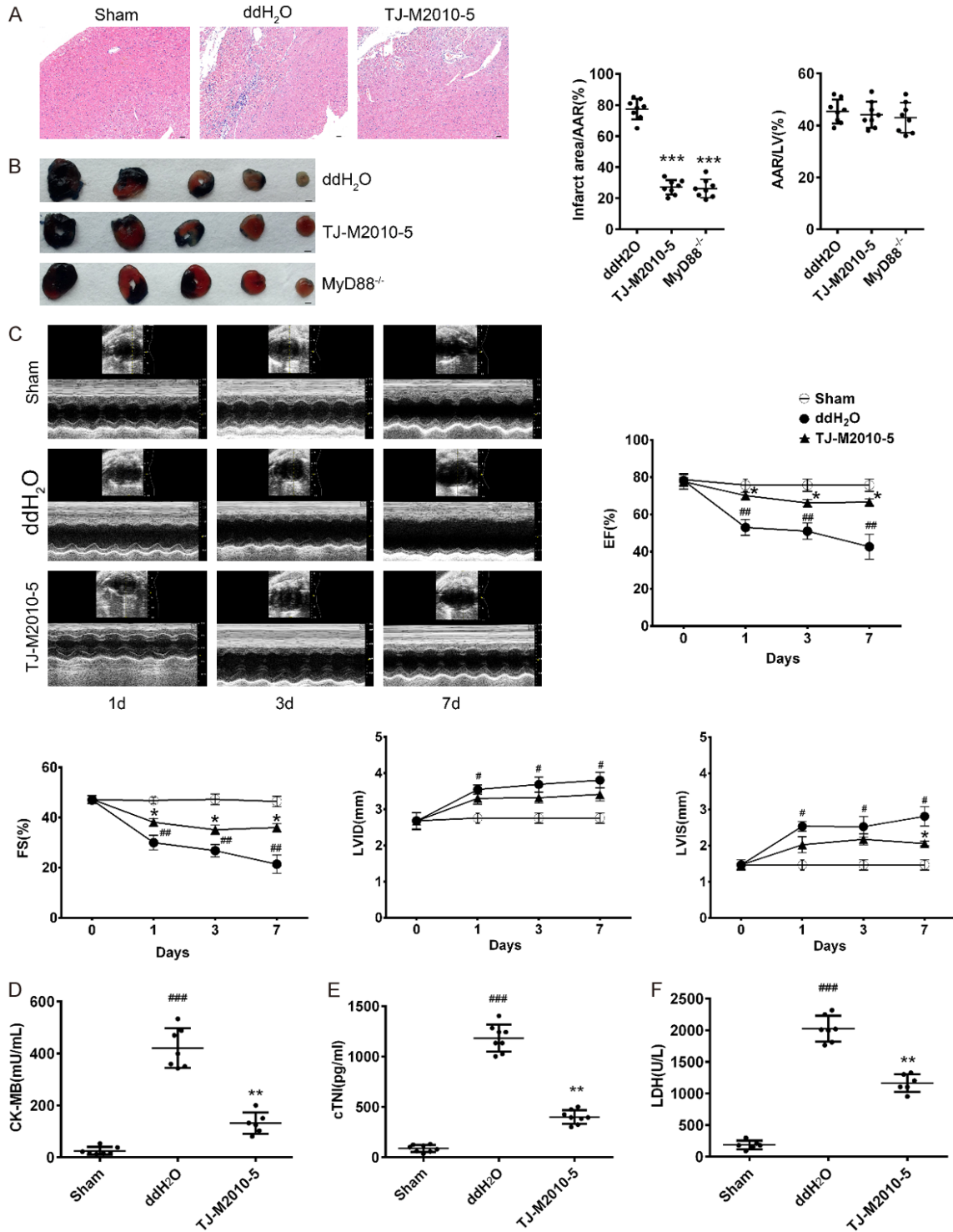
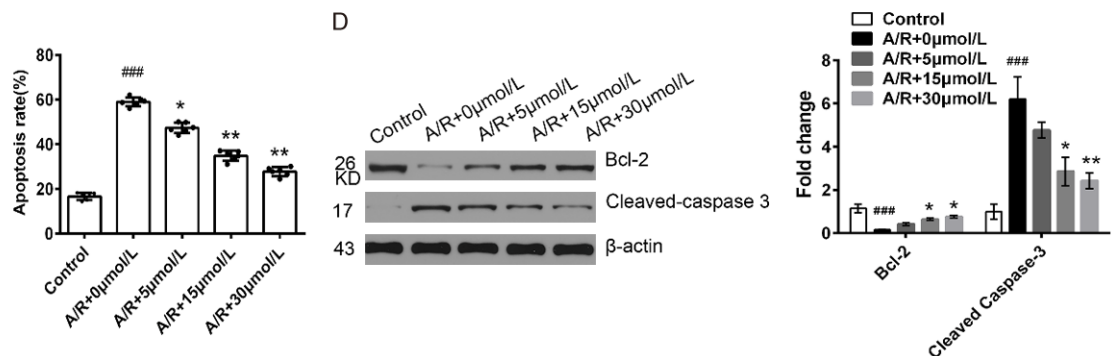
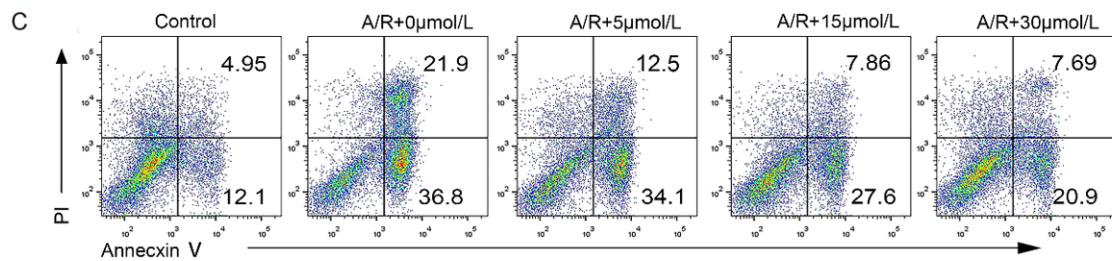
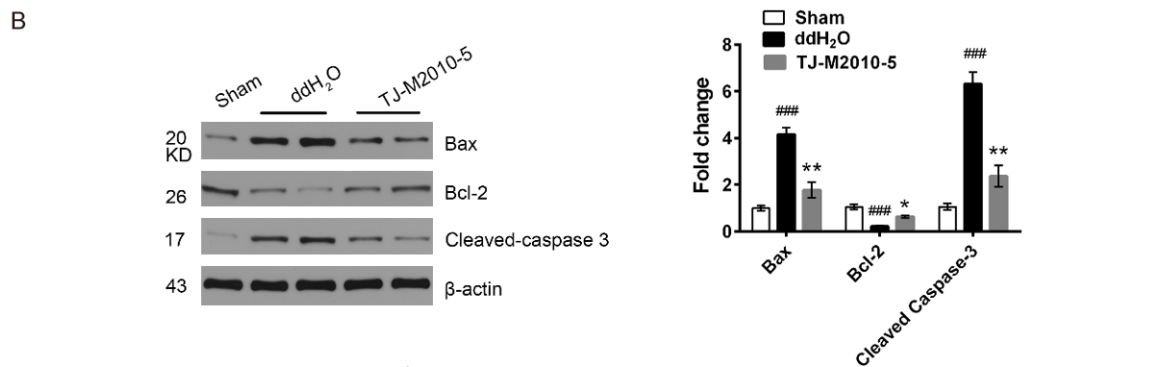
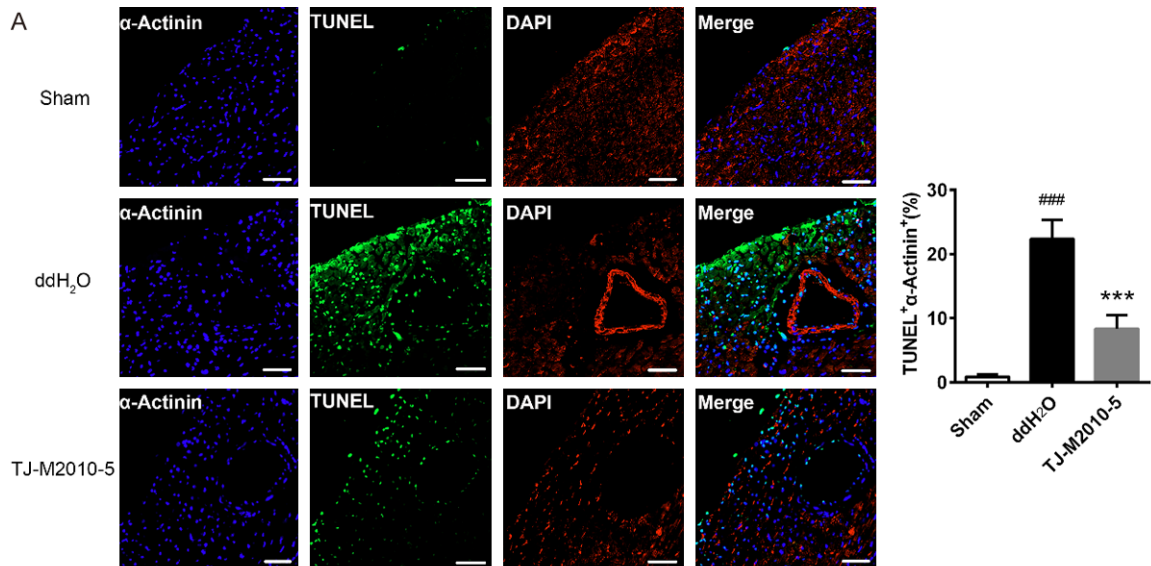


Figure 3. TJ-M2010-5 ameliorates pathology features and infarct area and protects the heart from MIRI. **A.** Heart tissues were collected 24 h after MIRI and stained with H&E (n = 6). Images are shown for each group. Original magnification, 200×; scale bar = 50 μm. Representative results for one of three independent experiments are shown. **B.** Mouse LV tissue sections stained with Evans blue and 2,3,5-triphenyltetrazolium chloride 24 h after ischemia reperfusion delineate AAR and infarcted regions (scale bar = 1 mm). AAR: LV and infarct area: AAR ratios were compared between ddH₂O and TJ-M2010-5 treatment groups or MyD88 knockout mice (n = 8). **C.** Echocardiography of LV ejection fraction (EF), LV fraction shortening (FS), LV dimensions at end-systole (LVIS), and LV dimensions at end-diastole (LVID) at 24 h, 3 d, and 7 d after ischemia reperfusion or sham surgery (n = 6-8) with representative

MyD88 inhibitor attenuates MIRI

M-mode echocardiographic images. D-F. Serum CK-MB, cTnl, and LDH levels in blood samples collected 24 h after MIRI (n = 6). Representative results for one of three independent experiments are shown. Data represent the means \pm SD. * $P < 0.05$, ** $P < 0.01$, *** $P < 0.001$ vs. ddH₂O; # $P < 0.05$, ## $P < 0.01$, ### $P < 0.001$ vs. sham; one-way ANOVA with Dunnett's post-hoc test.



MyD88 inhibitor attenuates MIRI

Figure 4. TJ-M2010-5 decreases IRI-induced cardiomyocyte apoptosis. Mice were exposed to 30-min ischemia followed by 24-h reperfusion. Cardiomyocytes were exposed to 3-h hypoxia and 3-h reoxygenation. (A) Representative photomicrographs of TUNEL and DAPI staining of cardiomyocytes (α -actinin) are shown ($n = 6$). Original magnification, 400 \times (bottom panel); scale bar = 50 μ m. Five random fields were selected. Heart tissues were harvested 24 h after ischemia reperfusion or sham operation. Semi-quantitative analysis of apoptotic area. The level of apoptosis was expressed as the % of TUNEL-positive area relative to total area. (B) Cleaved caspase-3, Bax, and Bcl-2 protein levels were analyzed by western blotting and densitometry using total proteins extracted from the heart 24 h after reperfusion. One of three independent experiments is shown. Density of the β -actin signal was divided by that of cleaved caspase-3, Bax, or Bcl-2 ($n = 6$). (C) Quantitative analysis of FCM results. Cardiomyocytes were pretreated with TJ-M2010-5 (0, 5, 15, or 30 μ mol/L), subjected to A/R, and stained with Annexin V and propidium iodide ($n = 6$). One of three independent experiments is shown. (D) Cleaved caspase-3 and Bcl-2 protein levels were analyzed by western blotting using total proteins extracted from cardiomyocytes after A/R. One of three independent experiments is shown. The density of the β -actin signal was divided by that of cleaved caspase-3 or Bcl-2 ($n = 6$). Data represent the means \pm SD. * $P < 0.05$, ** $P < 0.01$, *** $P < 0.001$ vs. ddH₂O, ### $P < 0.001$ vs. sham (A, B); * $P < 0.05$, ** $P < 0.01$ vs. A/R + 0 μ mol/L TJ-M2010-5, ### $P < 0.001$ vs. control (C, D); one-way ANOVA with Dunnett's post-hoc test.

TJ-M2010-5 ameliorates pathology features and infarct area and protects the heart from MIRI

We next performed H&E staining and echocardiography and evaluated infarct area, plasma lactate dehydrogenase (LDH), creatine kinase isoenzyme MB (CK-MB), and cardiac troponin I (cTnI) concentrations 24 h post-MIRI. Histopathological heart tissue slices of the MIRI group exhibited a wide range of focal myocardial lesions, cellular degeneration and necrosis, and inflammatory cell infiltration 24 h after MIRI. However, these pathological alterations were significantly ameliorated by TJ-M2010-5 pretreatment (**Figure 3A**). The extent of cardiac ischemic injury was compared at 24 h, 3 d, 7 d, and 14 d of reperfusion. Using similar areas at risk (AAR), the infarct area: AAR ratio was significantly lower in the TJ-M2010-5-treated mouse group and the MyD88-knockout mouse group than in the untreated group ($27.01 \pm 1.66\%$ vs. $77.38 \pm 2.34\%$, $26.13 \pm 2.07\%$ vs. $77.38 \pm 2.34\%$, respectively; **Figure 3B**). Compared with untreated mice, pretreatment with TJ-M2010-5 or knocking out MyD88 decreased the infarct area by nearly two-thirds. Echocardiography of TJ-M2010-5-treated mice revealed significant volumetric (μ L) decreases in left ventricular end-diastolic volume ($69.90 \pm 1.17 \mu$ L vs. $84.49 \pm 1.51 \mu$ L) and left ventricular end-systolic volume ($35.56 \pm 0.59 \mu$ L vs. $49.92 \pm 1.03 \mu$ L), increases in ejection fraction ($50.24 \pm 0.60\%$ vs. $40.91 \pm 0.73\%$), as well as improvements in LV diameters (end-diastolic, end-systolic, and fractional shortening) compared with those of wild-type mice after ischemia reperfusion (**Figure 3C**). Thus, TJ-M2010-5 pretreatment improved cardiac function.

Moreover, the significant upregulation in CK-MB, cTnI, and LDH levels in the MIRI group compared with the sham group ($P < 0.001$; **Figure 3D-F**) was attenuated at 24 h by TJ-M2010-5 pretreatment ($P < 0.001$).

TJ-M2010-5 attenuates IRI-induced cardiomyocyte apoptosis

Cardiomyocyte apoptosis plays a critical role in MIRI [22]. To explore the anti-apoptotic effect of TJ-M2010-5, we performed TUNEL with α -actinin staining and analyzed caspase-3 expression in heart tissue. TJ-M2010-5 pretreatment significantly reduced the number of apoptotic cardiomyocytes 24 h after MIRI (**Figures 4A** and **S1A**) and markedly downregulated cleaved caspase-3 and Bax levels, while upregulating Bcl-2 (**Figure 4B**). Moreover, FCM showed that TJ-M2010-5 pretreatment reduced neonatal rat cardiomyocyte apoptosis in a dose-dependent manner (**Figure 4C**). After A/R, cleaved caspase-3 levels decreased, whereas Bcl-2 levels increased in cardiomyocytes pretreated with TJ-M2010-5 compared with the ddH₂O group (**Figure 4D**).

TJ-M2010-5 inhibits leukocyte and monocyte infiltration in vivo

We isolated single mouse heart cells 24 h after MIRI and evaluated neutrophil and macrophage activation in each group by FCM. IHC indicated that there were considerably fewer myeloperoxidase (MPO) + neutrophils and F4/80+ macrophages in heart tissues of TJ-M2010-5-pretreated mice than in controls 24 h after MIRI (**Figure 5A**). Moreover, FCM demonstrated that levels of CD45+CD11b+Ly-6G+ neutrophils and CD45+CD11b+F4/80+ macrophages were

MyD88 inhibitor attenuates MIRI

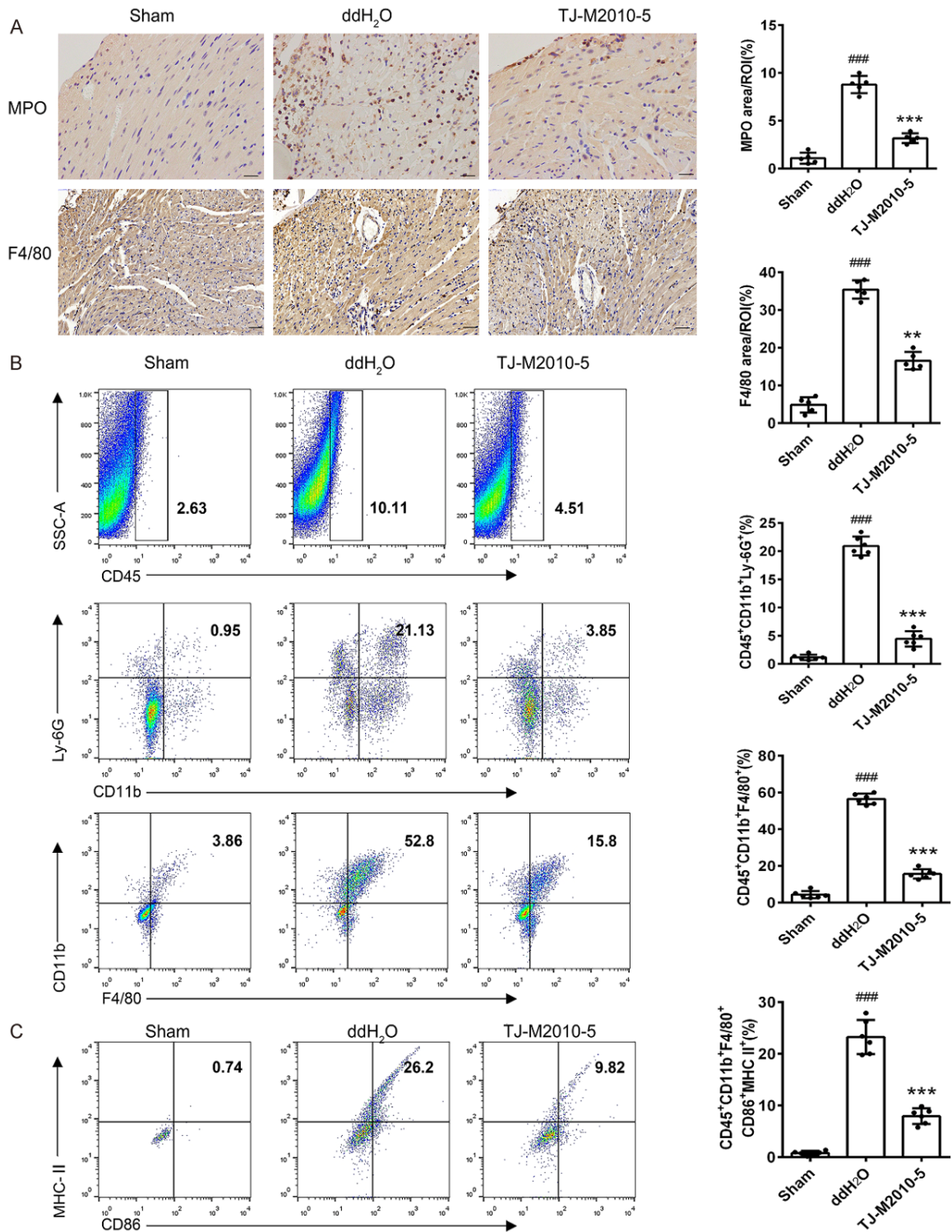
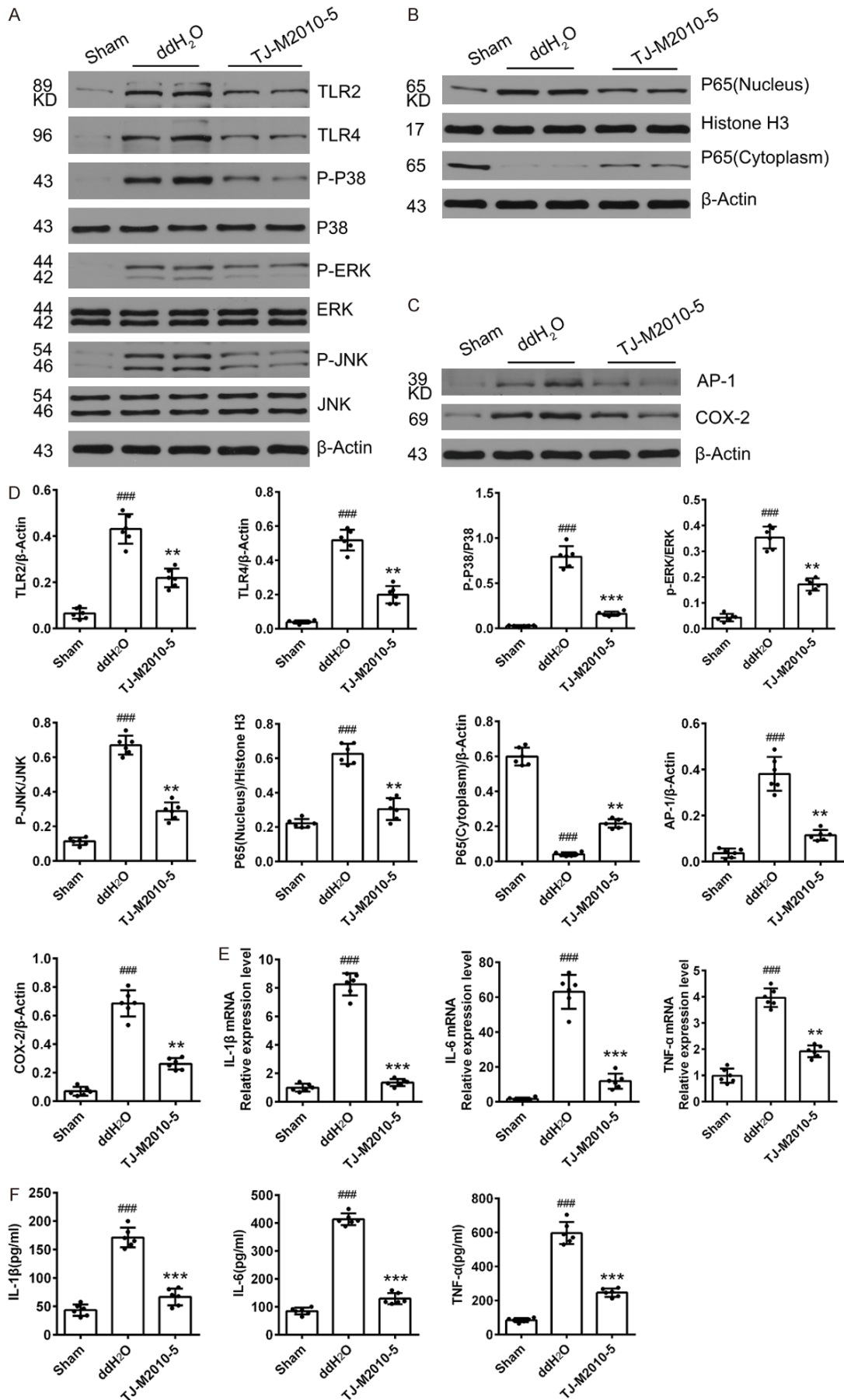


Figure 5. TJ-M2010-5 inhibits leukocyte and monocyte infiltration *in vivo*. A. IHC staining for MPO and F4/80 in heart sections 24 h post-induction (n = 6). Scale bar = 50 μ m; original magnification, 400 \times ; five fields were randomly selected. Semi-quantitative analysis of MPO+ and F4/80+ cells. B, C. Single cells were isolated from mouse hearts 24 h post-induction (n = 6-8). Frequencies of cardiac CD45+CD11b+Ly-6G+ neutrophils, CD45+CD11b+F4/80+ macrophages, and mature CD45+CD11b+F4/80+CD86+MHCII+ macrophages were determined by FCM. Data represent the means \pm SD. ** P < 0.01, *** P < 0.001 vs. ddH₂O; ### P < 0.001 vs. sham; one-way ANOVA with Dunnett's post-hoc test.

MyD88 inhibitor attenuates MIRI



MyD88 inhibitor attenuates MIRI

Figure 6. TJ-M2010-5 ameliorates inflammatory responses and downregulates TLR/MyD88 signaling after MIRI. A-C. Representative western blot analyses and summary showing protein levels of cardiac TLR2, TLR4, p-P38, p-ERK, p-JNK, AP-1, and COX2, plus NF- κ B nuclear translocation 24 h after MIRI or sham operation (n = 5-6; one of three independent experiments). D. Quantification of western blot results. The density of each internal reference signal was divided by that of its target protein. E. qRT-PCR results showing cardiac IL-1 β , TNF- α , and IL-6 mRNA levels 24 h after MIRI or sham operation (n = 6-8; one of three independent experiments). F. ELISA-based quantification of serum IL-1 β , TNF- α , and IL-6 levels (n = 6-8; one of three independent experiments). Data represent the means \pm SD. ** $P < 0.01$, *** $P < 0.001$ vs. ddH₂O; ### $P < 0.001$ vs. sham; one-way ANOVA with Dunnett's post-hoc test.

substantially lower in TJ-M2010-5-pretreated mice than in the ddH₂O group ($4.43 \pm 0.55\%$ vs. $20.91 \pm 0.68\%$, $15.60 \pm 1.05\%$ vs. $56.43 \pm 1.17\%$, respectively; **Figure 5B**). A comparable reduction in CD45+CD11b+F4/80+CD86+MHCII+ mature macrophage levels was also observed ($7.91 \pm 0.62\%$ vs. $23.25 \pm 1.34\%$ at 24 h; **Figure 5C**).

TJ-M2010-5 downregulates TLR/MyD88 signaling and ameliorates inflammatory responses in vivo after MIRI

DAMPs released during MIRI activate TLR/MyD88 signaling, which in turn induces NF- κ B nuclear translocation and generates cytokines that aggravate the inflammatory response [23]. TJ-M2010-5 pretreatment markedly downregulated TLR2, TLR4, p-P38, p-c-Jun N-terminal kinase (JNK), p-extracellular regulated protein kinases (ERK), and NF- κ B nuclear translocation in heart tissues (**Figure 6A, 6B, 6D**). We further evaluated inflammatory cytokine activator protein 1 (AP-1) and cyclooxygenase 2 (COX2) and found that TJ-M2010-5 significantly lowered AP-1 and COX2 levels (**Figure 6C and 6D**). Moreover, mRNA expression and serum concentrations of IL-1 β , IL-6, and TNF- α were substantially lower in the TJ-M2010-5 treatment group than in the IRI group (**Figure 6E and 6F**).

TJ-M2010-5 inhibits inflammatory responses, macrophagocyte activation, and migration in vitro

TJ-M2010-5 dramatically downregulated phosphorylation of P38, JNK, and ERK, as well as NF- κ B nuclear translocation in cardiomyocytes (**Figure 7A**). Moreover, IL-1 β and IL-6 mRNA expression and concentration in the supernatants were markedly lower in the TJ-M2010-5 pretreatment group than in the A/R group (**Figure 7B and 7C**).

Macrophages play vital roles in MIRI [24]; thus, to examine whether TJ-M2010-5 directly affects

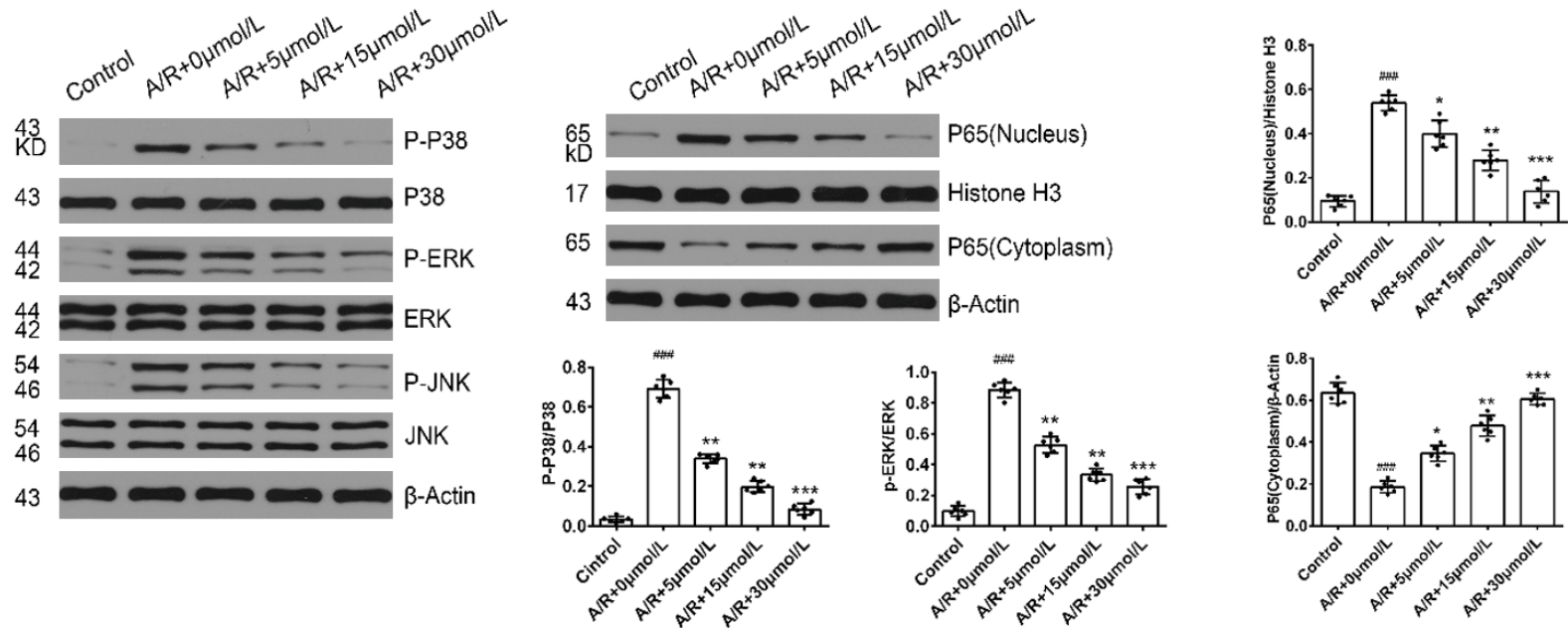
macrophage activation, we obtained BMDMs from mice and assessed the inhibitory effects of TJ-M2010-5 on the activation of A/R-exposed, cardiomyocyte supernatant-induced macrophages *in vitro*. Stimulation with the supernatants of A/R-treated cardiomyocytes upregulated CD80, CD86, and MHCII in BMDMs. In contrast, TJ-M2010-5 downregulated CD80, CD86, and MHCII in BMDMs in a dose-dependent manner. TJ-M2010-5 at 30 μ mol/L significantly inhibited BMDM activation (**Figure 7D**). TJ-M2010-5 also downregulated p-P38, p-JNK, and p-ERK, as well as NF- κ B nuclear translocation in macrophagocytes (**Figure 7E**). We further employed ELISA to measure IL-1 β , TNF- α , and IL-6 levels 24 h after stimulation with the supernatants of A/R-exposed cardiomyocytes with or without TJ-M2010-5 pretreatment. We found that these proinflammatory factors were downregulated by TJ-M2010-5 in a dose-dependent manner (**Figure S2A**). The effect of TJ-M2010-5 on macrophagocyte migration was evaluated by Transwell migration assays, which indicated that TJ-M2010-5 significantly suppressed macrophage migration in a dose-dependent manner, especially at 30 μ mol/L (**Figure S2B**).

TJ-M2010-5 attenuates cardiac fibrosis in vivo and fibroblast activation and migration in vitro

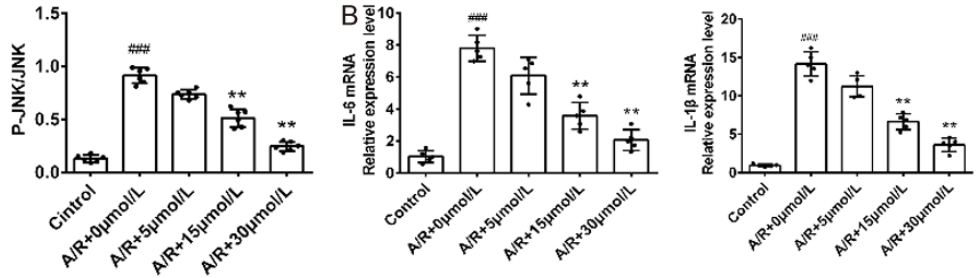
We next examined Masson's trichrome, collagen I, collagen III, and alpha-smooth muscle actin (α -SMA) staining via IHC 28 d post-MIRI. Heart tissues from the MIRI group presented with irregular morphologies, were disorganized, and had considerable fibrous hyperplasia. However, these pathological alterations were significantly ameliorated by TJ-M2010-5 pretreatment (**Figure 8A**). We further studied the effect of TJ-M2010-5 on collagens I and III, fibronectin, and α -SMA expression at the protein and mRNA level; both protein and mRNA levels were significantly upregulated in MIRI mouse hearts compared with those of the sham group and significantly downregulated

MyD88 inhibitor attenuates MIRI

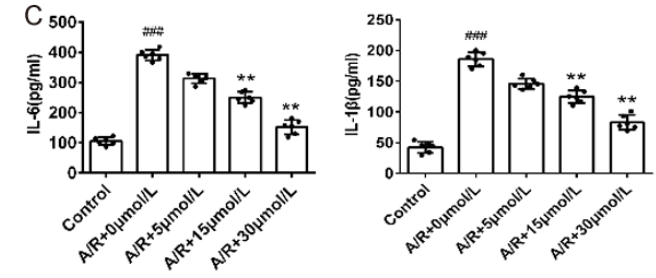
A



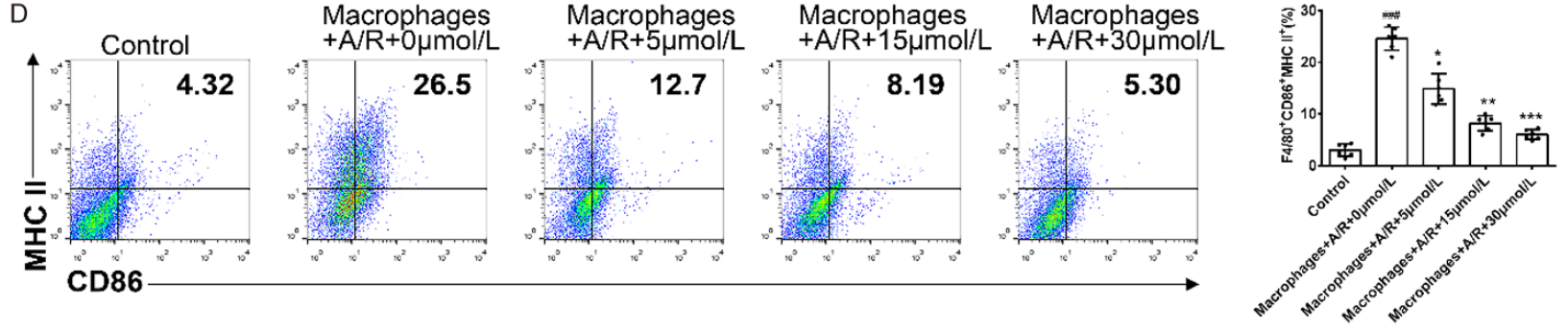
B



C



D



E

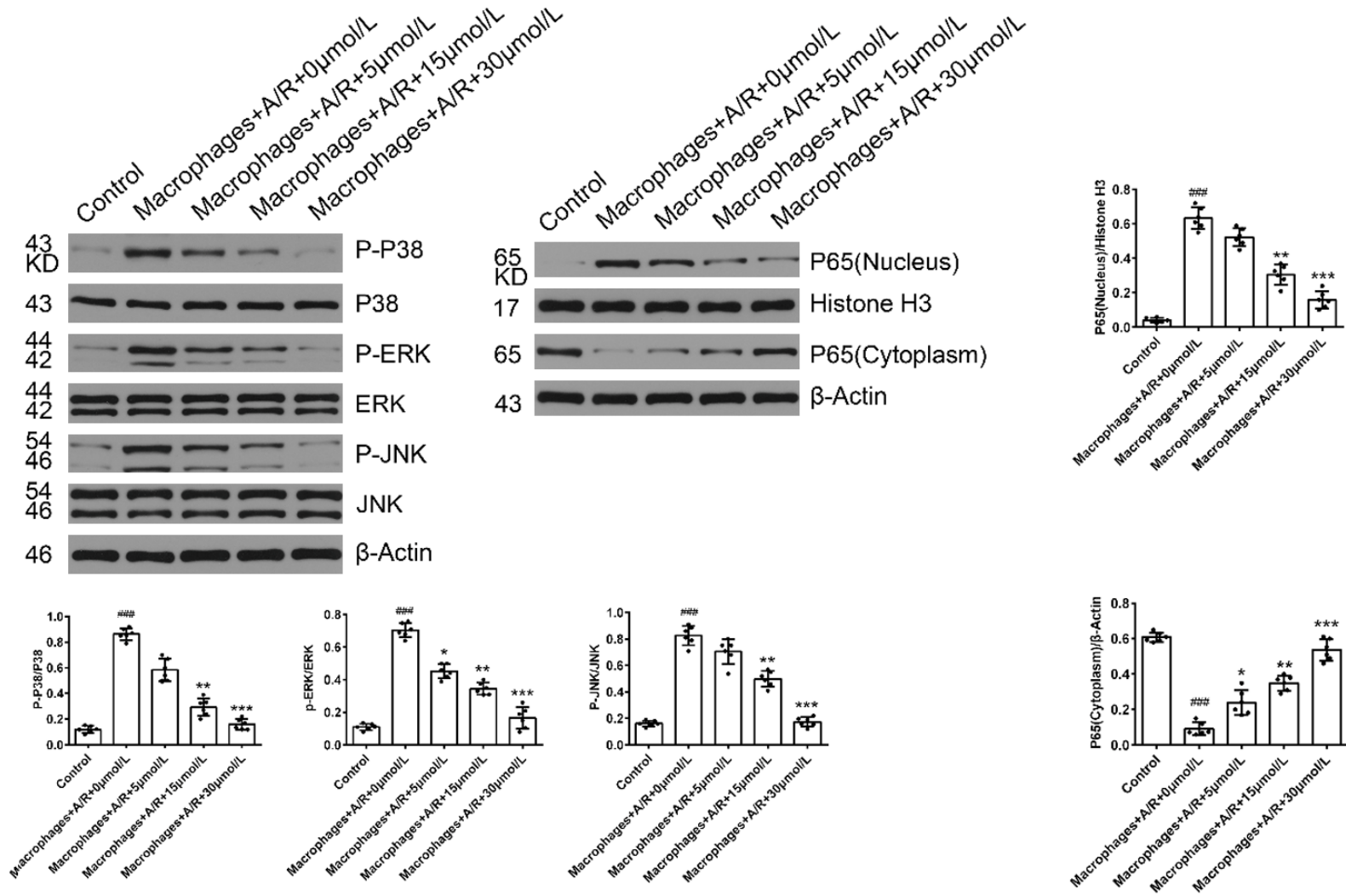


Figure 7. TJ-M2010-5 inhibits inflammatory responses, macrophages activation, and migration *in vitro*. (A) Representative western blot analyses and summary showing protein levels of p-P38, p-JNK, and p-ERK, as well as NF-κB nuclear translocation in A/R-exposed cardiomyocytes or controls (n = 5-6; one of three independent experiments). The density of each internal reference signal was divided by that of its target protein. (B) IL-1β and IL-6 mRNA levels in cardiomyocytes exposed to A/R injury or control (n = 5-6; one of three independent experiments) were measured by qRT-PCR. (C) IL-1β and IL-6 levels in cardiomyocyte culture supernatants were quantified by ELISA (n = 6-8; one of three independent experiments). (D) Macrophages were stained with anti-F4/80, anti-CD86, and anti-MHCII antibodies. The ratio of CD86+MHCII+F4/80+ cells was measured by FCM (n = 3; one of three independent experiments). (E) Representative western blot analyses and summary showing protein levels of p-P38, p-JNK, and p-ERK, as well as NF-κB nuclear translocation in macrophagocytes subjected to supernatants of A/R-exposed cardiomyo-

MyD88 inhibitor attenuates MIRI

cytes or control (n = 5-6; one of three independent experiments). The density of each internal reference signal was divided by that of its target protein. Data represent the means \pm SD. ** $P < 0.01$, *** $P < 0.001$ vs. A/R + 0 $\mu\text{mol/L}$ TJ-M2010-5 (A-C); * $P < 0.05$, ** $P < 0.01$, *** $P < 0.001$ vs. macrophages + A/R + 0 $\mu\text{mol/L}$ TJ-M2010-5 (D, E); **** $P < 0.001$ vs. control; one-way ANOVA with Dunnett's post-hoc test.

after TJ-M2010-5 treatment (Figures 8B and S3A). Furthermore, we incubated fibroblasts with the supernatant of cardiomyocytes subjected to hypoxia and reoxygenation and then analyzed the effect of TJ-M2010-5 on α -SMA expression. Both α -SMA protein and mRNA levels increased in the A/R group and decreased in response to TJ-M2010-5 pretreatment (Figures 8C, S3B and S1B). Finally, we performed Transwell migration assays and found that TJ-M2010-5 significantly inhibited fibroblast migration in a dose-dependent manner, especially at 30 $\mu\text{mol/L}$ (Figure 8D).

Discussion

In the present study, we demonstrated that MyD88 plays a vital role in MIRI damage and repair and that the MyD88 inhibitor TJ-M2010-5 mitigates MIRI. This inhibitor ameliorated MIRI, reduced cardiomyocyte apoptosis, suppressed CD80+CD86+MHCII+ macrophage activation and the release of proinflammatory cytokines, and diminished CD11b+Ly-6G+ neutrophil infiltration. Furthermore, TJ-M2010-5 decreased fibroblast activation, which is responsible for cardiac remodeling.

MyD88 is an important adapter protein of all TLRs, except for TLR3, and its activation induces cytoplasmic signaling cascades that stimulate NF- κ B and MAPK signaling and trigger inflammation [25]. Indeed, TLR/MyD88 signaling was found to regulate inflammation and tissue repair in response to MIRI [26]. Moreover, previous reports demonstrated that MyD88 overexpression results in cardiac dysfunction. In MyD88^{-/-} mice with MIRI, neutrophil infiltration, proinflammatory factor induction, and myocardial infarct area were significantly reduced compared with those of wild-type mice [23, 27, 28]. Here, we observed significant MyD88 upregulation in the myocardium during MIRI starting as early as 12 h, peaking at 24 h, and lasting for \leq 28 d. Thus, MyD88 participates in both the early and late stages of MIRI. Double immunofluorescence revealed that α -actinin+, F4/80+, and vimentin+ cells in the heart express MyD88 after ischemia reperfu-

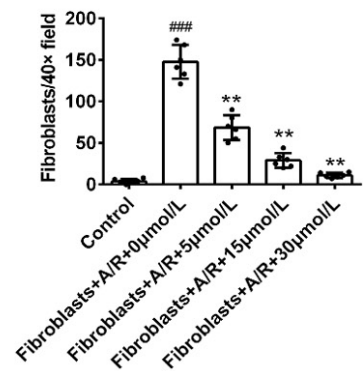
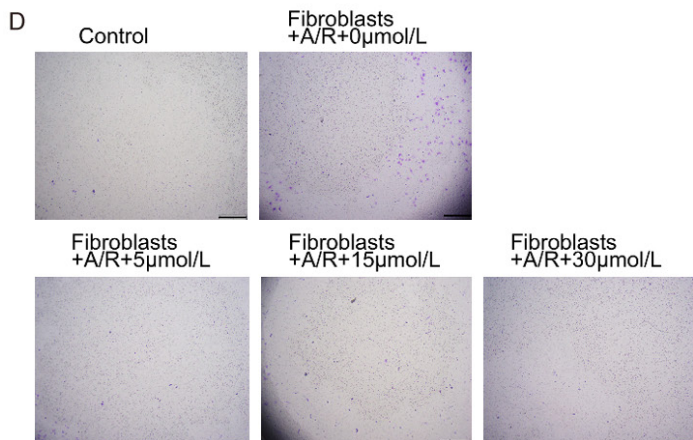
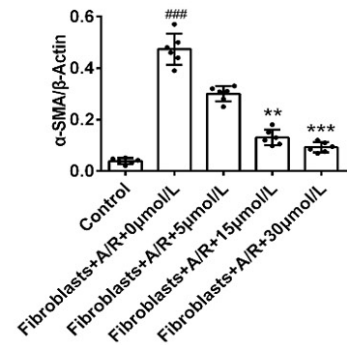
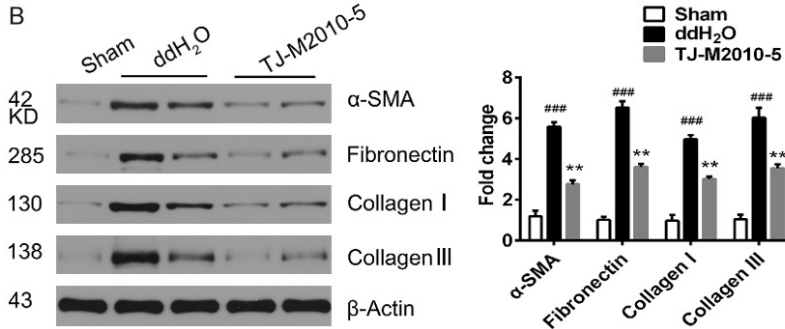
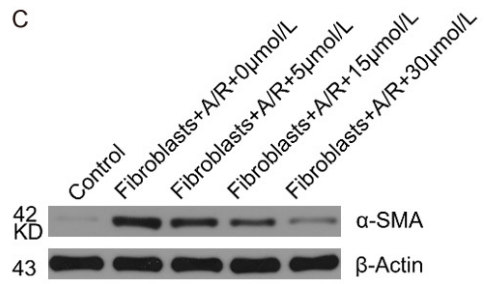
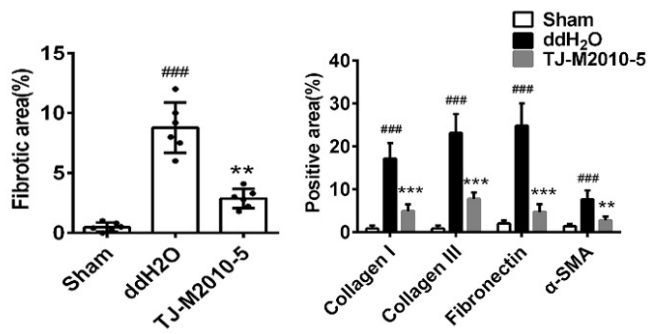
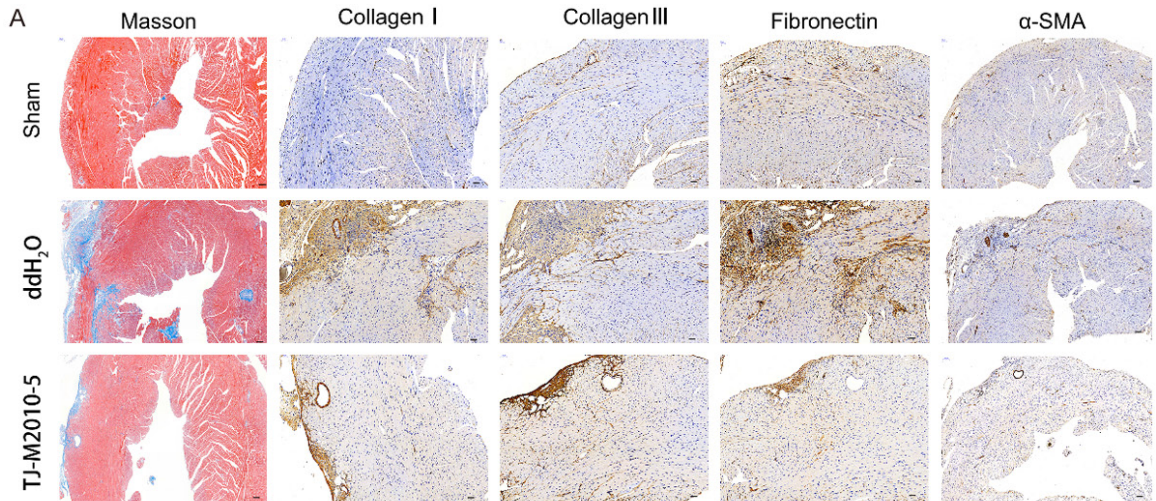
sion. Therefore, MyD88 is a potential target molecule for MIRI treatment.

Current studies often apply gene knockout or silencing. However, these techniques are difficult to implement at the clinical level. Here, we observed in H9C2 cells that TJ-M2010-5 inhibits MyD88 dimerization by interfering with its homodimerization and TIRAP-MyD88 heterodimerization. We also demonstrated the anti-MIRI effect of TJ-M2010-5 in MIRI murine and cardiomyocyte A/R models. Inhibition of MyD88 activation by TJ-M2010-5 improved the cardiac function index and decreased myocardial enzyme levels. H&E and IHC staining of heart tissue corroborated the cardioprotective effect of TJ-M2010-5. Nevertheless, further investigations are required to determine the detailed mechanism by which TJ-M2010-5 affects MIRI.

During the early phases of MIRI, macrophages and cardiomyocytes release proinflammatory cytokines such as IL-1 β , IL-6, and TNF- α , which recruit neutrophils and other macrophages and aggravate cardiomyocyte apoptosis [6, 29, 30]. MyD88 was also found highly expressed in cardiomyocytes in an extracellular HSP60-induced MIRI model [31]. In agreement, our immunofluorescence and western blotting results demonstrated that MyD88 is upregulated in macrophagocytes and cardiomyocytes both *in vivo* and *in vitro*. Pretreatment with the MyD88 inhibitor inhibited CD45+CD11b+Ly-6G+ and CD45+CD11b+F4/80+ cell infiltration; TLR2, TLR4, cleaved caspase-3, Bax, Bcl-2, AP-1, and COX2 expression; NF- κ B nuclear translocation; and P38, JNK, and ERK phosphorylation in the heart 24 h after MIRI. TJ-M2010-5 also reduced the number of activated macrophages. Coculturing with TJ-M2010-5 after A/R stimulation markedly inhibited cardiomyocyte apoptosis and BMDM activation in a dose-dependent manner.

Heart remodeling is the final effect of MIRI [32], with fibroblasts playing a key role in this process [33]. In the infarcted myocardium, the release of DAMPs by necrotic cardiomyocytes and macrophagocytes triggers an inflammation-driven fibrotic response known as the

MyD88 inhibitor attenuates MIRI



MyD88 inhibitor attenuates MIRI

Figure 8. TJ-M2010-5 alleviates myocardial fibrosis in mice after MIRI *in vivo* and fibroblast activation and migration *in vitro*. (A) Heart tissues were collected 28 d after IRI and stained with Masson's trichrome for fibronectin, collagens I and III, and α -SMA (n = 6). Original magnification 400 \times ; scale bar = 50 μ m. Five fields were randomly selected. Semi-quantitative analysis of the fibrotic area by Masson's trichrome staining. Semi-quantitative analysis of positive areas for fibronectin, collagens I and III, and α -SMA. (B) The effect of TJ-M2010-5 on cardiac protein expression of fibronectin, collagens I and III, and α -SMA was analyzed by western blotting (n = 6; one of three independent experiments). Densitometry of proteins relative to β -actin as an internal control. (C) α -SMA protein levels in fibroblasts subjected to supernatants of A/R-exposed cardiomyocytes or control were analyzed by western blotting in three independent experiments. The density of β -actin was divided by α -SMA (n = 6). (D) Numbers of migrated fibroblasts were evaluated by the Transwell migration assay (n = 6). Original magnification 40 \times ; scale bar = 500 μ m. Five discontinuous fields were randomly selected. Data represent the means \pm SD. ** P < 0.01, *** P < 0.001 vs. ddH₂O; ### P < 0.001 vs. sham (A, B); ** P < 0.01, *** P < 0.001 vs. fibroblasts + A/R + 0 μ mol/L; ### P < 0.001 vs. control (C); one-way ANOVA with Dunnett's post-hoc test.

DAMPs/fibroblast axis [34]. A cytokine-rich environment that includes TNF- α , IL-1 β , and IL-6 forms after cardiac injury, activates fibroblasts, increases their migration, induces them to differentiate into myofibroblasts with elevated α -SMA expression, and enhances collagen expression and secretion. The latter fills in the areas devoid of cardiomyocytes and prevents myocardial wall rupture but causes fibrosis [35-37]. In the present study, we found that cardiac vimentin+ cells highly expressed MyD88 after a 7-day ischemia. TJ-M2010-5 pretreatment decreased cardiac P38, JNK, and ERK phosphorylation after 7 d of MIRI. It also reduced the area of fibrosis and the expression levels of fibronectin, α -SMA, collagen I, and collagen III after 28 days of MIRI. Moreover, we confirmed that TJ-M2010-5 pretreatment reduced fibroblast migration and P38, JNK, and ERK phosphorylation via a MyD88-dependent pathway.

Nevertheless, this study has some limitations. We only studied the effects of the drug on BMDMs but did not evaluate the tissue-resident macrophages. Our research on fibroblasts focused on the effects promoted by hypoxic and reoxygenated cardiomyocytes. In fact, the stimuli for the activation of fibroblasts are so complex that we cannot accurately mimic the myocardial ischemia reperfusion environment that occurs *in vivo*.

In conclusion, the present study indicates that the MyD88 inhibitor TJ-M2010-5 may reverse nearly two-thirds of the infarct area in MIRI by effectively reducing the inflammatory response and cardiac fibrosis caused by MIRI. Our findings provide new insights into targeted treatments for MIRI; however, further validation in clinical studies is needed to assess the effects of TJ-M2010-5 on MIRI.

Acknowledgements

We would like to thank Dr. Maria-Luisa Alegre in the University of Chicago for providing C57BL/6 MyD88^{-/-} mice. We would also like to thank Dr. Ying Xiang for assistance with flow cytometry; Dr. Xia Huang and Lin Xie for guiding surgery on mice; and Editage for English language editing. This work was supported by the National Natural Science Foundation of China [grant number 81672946]. The authors declare no competing financial interests.

Disclosure of conflict of interest

None.

Abbreviations

AAR, areas at risk; AP-1, activator protein 1; A/R, anoxia/reoxygenation; α -SMA, alpha-smooth muscle actin; Bcl-2, B-cell lymphoma 2; BMDM, bone marrow-derived macrophage; Brd, U bromodeoxyuridine; CK-MB, creatine kinase isoenzyme MB; COX2, cyclooxygenase 2; cTnI, cardiac troponin I; DAMPs, danger-associated molecular patterns; DAPI, 4',6-diamidino-2-phenylindole; DMEM, Dulbecco's modified Eagle's medium; ERK, extracellular regulated protein kinase; FBS, fetal bovine serum; FCM, flow cytometry; H&E, hematoxylin and eosin; IHC, immunohistochemistry; IL-1 β , interleukin-1-beta; IL-6, interleukin-6; i.p., intraperitoneal injection; IRI, ischemia/reperfusion injury; JNK, c-Jun N-terminal kinase; LDH, lactate dehydrogenase; LV, left ventricle; MAPK, mitogen-activated protein kinase; M-CSF, macrophage colony-stimulating factor; MHCII, major histocompatibility complex class II; MIRI, myocardial ischemia/reperfusion injury; MPO, myeloperoxidase; MyD88, myeloid differentiation primary response 88; NF- κ B, nuclear factor kappa-light-

chain-enhancer of activated B cells; TIR, Toll interleukin-1 receptor; TIRAP, TIR domain-containing adaptor protein; TLR, Toll-like receptor; TNF- α , tumor necrosis factor-alpha; TRAF6, TNF receptor-associated factor 6; TUNEL, terminal deoxynucleotidyl transferase-mediated nick-end labeling.

Address correspondence to: Drs. Ping Zhou and Dunfeng Du, Institute of Organ Transplantation, Tongji Hospital, Tongji Medical College, Huazhong University of Science and Technology, 1095 Jiefang Road, Wuhan 430030, Hubei, China. E-mail: pzhou@tjh.tjmu.edu.cn (PZ); dfdu@tjh.tjmu.edu.cn (DFD); Dr. Fengchao Jiang, Academy of Pharmacy, Tongji Medical College, Huazhong University of Science and Technology, 1095 Jiefang Road, Wuhan 430030, Hubei, China. E-mail: fengchao@mails.tjmu.edu.cn

References

- [1] GBD 2015 DALYs and HALE Collaborators. Global, regional, and national disability-adjusted life-years (DALYs) for 315 diseases and injuries and healthy life expectancy (HALE), 1990-2015: a systematic analysis for the global burden of disease study 2015. *Lancet* 2016; 388: 1603-1658.
- [2] Wu Y, Li S, Patel A, Li X, Du X, Wu T, Zhao Y, Feng L, Billot L, Peterson ED, Woodward M, Kong L, Huo Y, Hu D, Chalkidou K and Gao R; CPACS-3 Investigators. Effect of a quality of care improvement initiative in patients with acute coronary syndrome in resource-constrained hospitals in China: a randomized clinical trial. *JAMA Cardiol* 2019; 4: 418-427.
- [3] Farah A and Barbagelata A. Unmet goals in the treatment of acute myocardial infarction: review. *F1000Res* 2017; 6: F1000 Faculty Rev-1243.
- [4] Yellon DM and Hausenloy DJ. Myocardial reperfusion injury. *N Engl J Med* 2007; 357: 1121-1135.
- [5] Timmers L, Pasterkamp G, de Hoog VC, Arslan F, Appelman Y and de Kleijn DP. The innate immune response in reperfused myocardium. *Cardiovasc Res* 2012; 94: 276-283.
- [6] Wei L. Toll-like receptor signaling a critical modulator of cell survival and ischemic injury in the heart. *Am J Physiol Heart Circ Physiol* 2008; 296: H1-H12.
- [7] Sun Y, Liu WZ, Liu T, Feng X, Yang N and Zhou HF. Role of toll-like receptors in myocardial infarction. *J Recept Signal Transduct Res* 2015; 35: 420-422.
- [8] Fang Y and Hu J. Toll-like receptor and its roles in myocardial ischemic reperfusion injury. *Med Sci Monit* 2011; 17: RA100-9.
- [9] Turner NA. Inflammatory and fibrotic responses of cardiac fibroblasts to myocardial damage associated molecular patterns (DAMPs). *J Mol Cell Cardiol* 2016; 94: 189-200.
- [10] Chen W and Frangogiannis NG. Fibroblasts in post-infarction inflammation and cardiac repair. *Biochim Biophys Acta* 2013; 1833: 945-953.
- [11] Warner N and Nunez G. MyD88: a critical adaptor protein in innate immunity signal transduction. *J Immunol* 2013; 190: 3-4.
- [12] Hardiman G, Rock FL, Balasubramanian S, Kastelein RA and Bazan JF. Molecular characterization and modular analysis of human MyD88. *Oncogene* 1996; 13: 2467-2475.
- [13] Arslan F, de Kleijn DP and Pasterkamp G. Innate immune signaling in cardiac ischemia. *Nat Rev Cardiol* 2011; 8: 292-300.
- [14] Epelman S, Liu PP and Mann DL. Role of innate and adaptive immune mechanisms in cardiac injury and repair. *Nat Rev Immunol* 2015; 15: 117-129.
- [15] Vilahur G and Badimon L. Ischemia/reperfusion activates myocardial innate immune response: the key role of the toll-like receptor. *Front Physiol* 2014; 5: 496.
- [16] Gombozhapova A, Rogovskaya Y, Shurupov V, Rebenkova M, Kzhyshkowska J, Popov SV, Karpov RS and Ryabov V. Macrophage activation and polarization in post-infarction cardiac remodeling. *J Biomed Sci* 2017; 24: 13.
- [17] Li C, Zhang LM, Zhang X, Huang X, Liu Y, Li MQ, Xing S, Yang T, Xie L, Jiang FC, Jiang HY, He WT and Zhou P. Short-term pharmacological inhibition of MyD88 homodimerization by a novel inhibitor promotes robust allograft tolerance in mouse cardiac and skin transplantation. *Transplantation* 2017; 101: 284-293.
- [18] Ding Z, Du D, Yang Y, Yang M, Miao Y, Zou Z, Zhang X, Li Z, Zhang X, Zhang L, Wang X, Zhao Y, Jiang J, Jiang F and Zhou P. Short-term use of MyD88 inhibitor TJ-M2010-5 prevents d-galactosamine/lipopolysaccharide-induced acute liver injury in mice. *Int Immunopharmacol* 2019; 67: 356-365.
- [19] Xie L, Jiang FC, Zhang LM, He WT, Liu JH, Li MQ, Zhang X, Xing S, Guo H and Zhou P. Targeting of MyD88 homodimerization by novel synthetic inhibitor TJ-M2010-5 in preventing colitis-associated colorectal cancer. *J Natl Cancer Inst* 2016; 108: djv364.
- [20] Xu Z, Alloush J, Beck E and Weisleder N. A murine model of myocardial ischemia-reperfusion injury through ligation of the left anterior descending artery. *Methods Mol Biol* 2014; e51329.
- [21] Watkins SJ, Borthwick GM and Arthur HM. The H9C2 cell line and primary neonatal cardiomyocyte cells show similar hypertrophic re-

MyD88 inhibitor attenuates MIRI

- sponses in vitro. *In Vitro Cell Dev Biol Anim* 2011; 47: 125-131.
- [22] Teringova E and Tousek P. Apoptosis in ischemic heart disease. *J Transl Med* 2017; 15: 87.
- [23] Feng Y, Zhao H, Xu X, Buys ES, Raheer MJ, Bopassa JC, Thibault H, Scherrer-Crosbie M, Schmidt U and Chao W. Innate immune adaptor MyD88 mediates neutrophil recruitment and myocardial injury after ischemia-reperfusion in mice. *Am J Physiol Heart Circ Physiol* 2008; 295: H1311-H1318.
- [24] Epelman S, Lavine KJ and Randolph GJ. Origin and functions of tissue macrophages. *Immunity* 2014; 41: 21-35.
- [25] Siednienko J, Gajanayake T, Fitzgerald KA, Moynagh P and Miggin SM. Absence of MyD88 results in enhanced TLR3-dependent phosphorylation of IRF3 and increased IFN-beta and RANTES production. *J Immunol* 2011; 186: 2514-2522.
- [26] Kay E, Scotland RS and Whiteford JR. Toll-like receptors: role in inflammation and therapeutic potential. *Biofactors* 2014; 40: 284-294.
- [27] Chen W, Huang Z, Jiang X, Li C and Gao X. Overexpression of myeloid differentiation protein 88 in mice induces mild cardiac dysfunction, but no deficit in heart morphology. *Braz J Med Biol Res* 2016; 49: e4794.
- [28] Feng Y, Zou L, Chen C, Li D and Chao W. Role of cardiac- and myeloid-MyD88 signaling in endotoxin shock. *Anesthesiology* 2014; 121: 1258-1269.
- [29] Chen B and Frangogiannis NG. Immune cells in repair of the infarcted myocardium. *Microcirculation* 2017; 24.
- [30] Blyszczuk P, Kania G, Dieterle T, Marty RR, Valaperti A, Berthonneche C, Pedrazzini T, Berger CT, Dirnhofer S, Matter CM, Penninger JM, Lüscher TF and Eriksson U. Myeloid differentiation factor-88/interleukin-1 signaling controls cardiac fibrosis and heart failure progression in inflammatory dilated cardiomyopathy. *Circ Res* 2009; 105: 912-920.
- [31] Tian J, Guo X, Liu XM, Liu L, Weng QF, Dong SJ, Knowlton AA, Yuan WJ and Lin L. Extracellular HSP60 induces inflammation through activating and up-regulating TLRs in cardiomyocytes. *Cardiovasc Res* 2013; 98: 391-401.
- [32] Frangogiannis NG. Cardiac fibrosis: cell biological mechanisms, molecular pathways and therapeutic opportunities. *Mol Aspects Med* 2019; 65: 70-99.
- [33] Porter KE and Turner NA. Cardiac fibroblasts: at the heart of myocardial remodeling. *Pharmacol Ther* 2009; 123: 255-278.
- [34] Zhang W, Lavine KJ, Epelman S, Evans SA, Weinheimer CJ, Barger PM and Mann DL. Necrotic myocardial cells release damage-associated molecular patterns that provoke fibroblast activation in vitro and trigger myocardial inflammation and fibrosis in vivo. *J Am Heart Assoc* 2015; 4: e001993.
- [35] van Nieuwenhoven FA and Turner NA. The role of cardiac fibroblasts in the transition from inflammation to fibrosis following myocardial infarction. *Vascul Pharmacol* 2013; 58: 182-188.
- [36] Nielsen SH, Mouton AJ, DeLeon-Pennell KY, Genovese F, Karsdal M and Lindsey ML. Understanding cardiac extracellular matrix remodeling to develop biomarkers of myocardial infarction outcomes. *Matrix Biol* 2019; 75-76: 43-57.
- [37] Wang JW, Fontes MSC, Wang X, Chong SY, Kessler EL, Zhang YN, de Haan JJ, Arslan F, de Jager SCA, Timmers L, van Veen TAB, Lam CSP and Kleijn DPV. Leukocytic Toll-like receptor 2 deficiency preserves cardiac function and reduces fibrosis in sustained pressure overload. *Sci Rep* 2017; 7: 9193.

MyD88 inhibitor attenuates MIRI

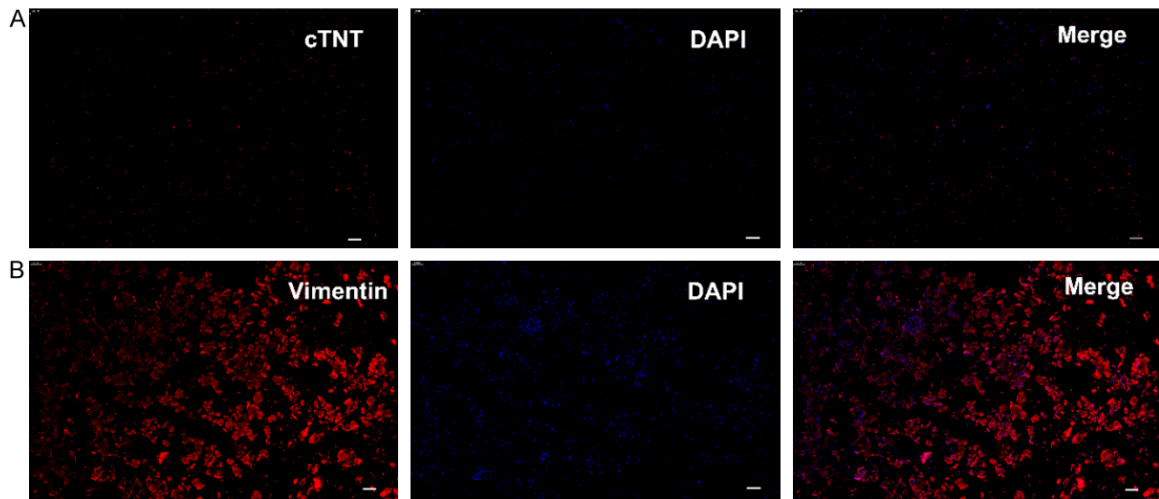


Figure S1. Identification of primary cardiomyocytes and fibroblasts. A. Immunofluorescence staining of cTnT for primary cardiomyocytes (n = 6; one of three independent experiments). B. Immunofluorescence staining of vimentin for fibroblasts that underwent two passages (n = 6; one of three independent experiments). Scale bar = 200 μ m; original magnification 100 \times ; five fields were randomly selected.

MyD88 inhibitor attenuates MIRI

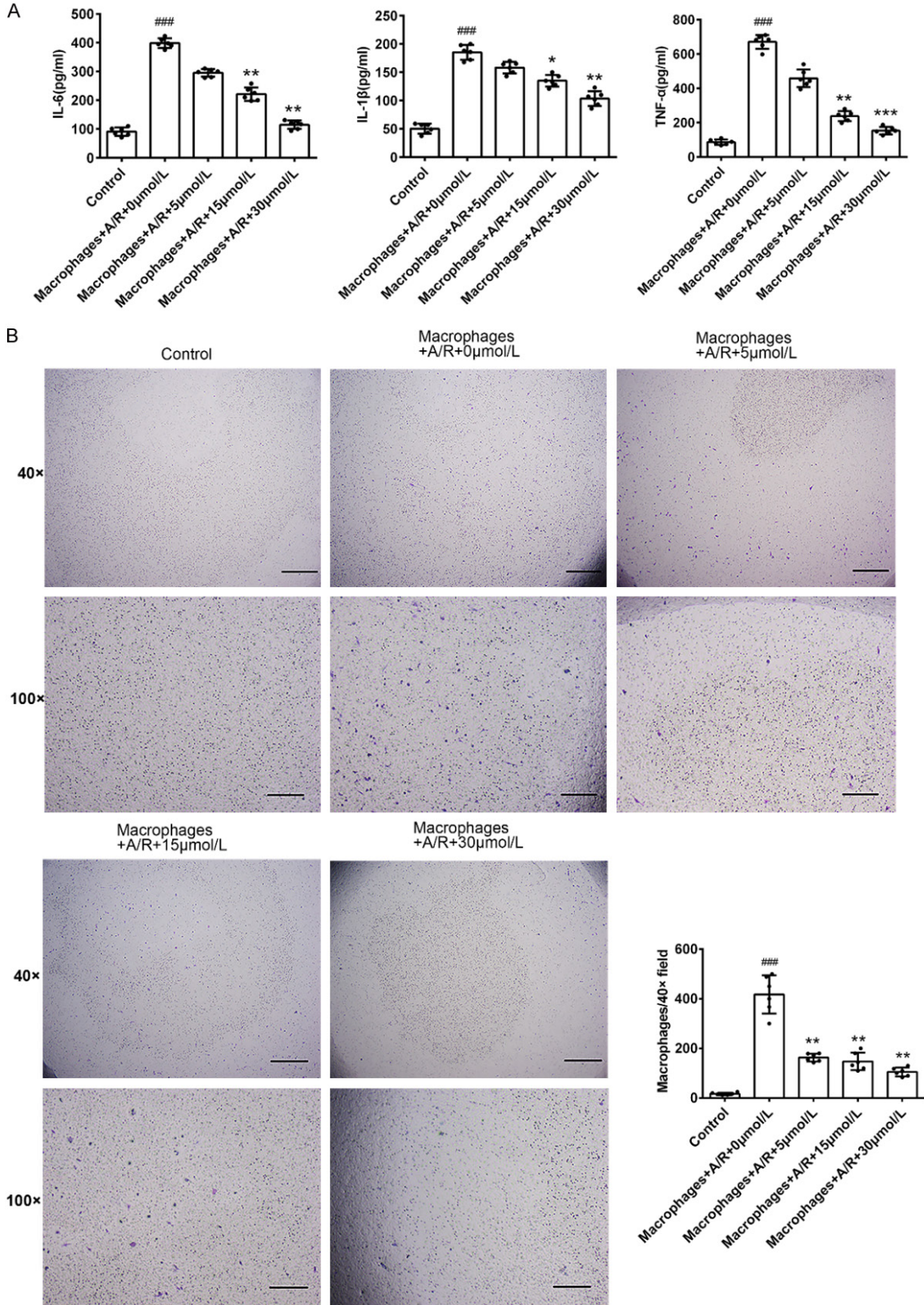


Figure S2. ELISA and migration results of macrophages *in vitro*. A. IL-6, IL-1 β , and TNF- α levels in macrophagocyte supernatant were quantified by ELISA (n = 5-6; one of three independent experiments). B. Macrophagocyte migration was evaluated by Transwell migration assays (n = 6). Original magnification, 40 \times (top panel); scale bar = 500 μ m. Magnified view, 100 \times (bottom panel); scale bar = 200 μ m. Five discontinuous fields were randomly selected.

MyD88 inhibitor attenuates MIRI

Data represent the means \pm SD. * $P < 0.05$, ** $P < 0.01$, *** $P < 0.001$ vs. macrophages + A/R + 0 $\mu\text{mol/L}$ TJ-M2010-5; ### $P < 0.001$ vs. control; one-way ANOVA with Dunnett's post-hoc test.

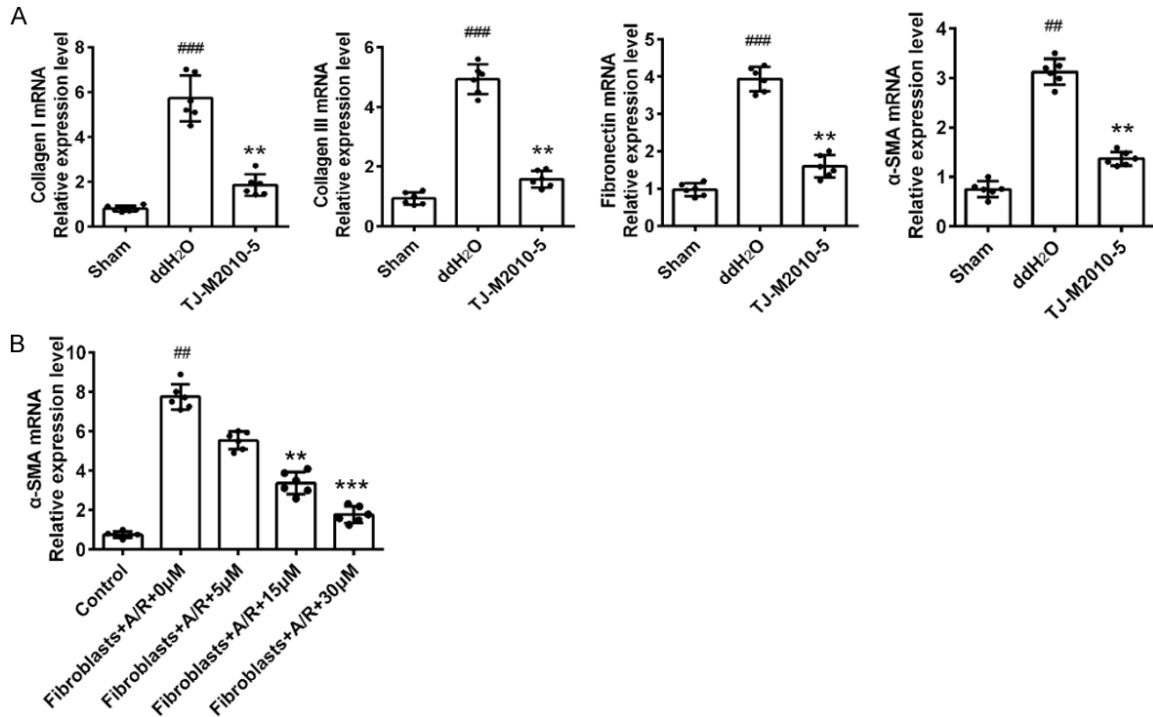


Figure S3. qRT-PCR results of fibrosis *in vivo* and *in vitro*. (A) Effects of TJ-M2010-5 on cardiac mRNA levels of collagens I and III, fibronectin and α -SMA ($n = 5-6$; one of three independent experiments). (B) α -SMA mRNA levels in fibroblasts subjected to supernatants of A/R-exposed cardiomyocytes or control ($n = 5-6$; one of three independent experiments). Data represent the means \pm SD. ** $P < 0.01$ vs. ddH₂O; ### $P < 0.001$ vs. sham (A); ** $P < 0.01$ vs. fibroblasts + A/R + 0 μM ; ### $P < 0.001$ vs. control (B); one-way ANOVA with Dunnett's post-hoc test.